Focus issue introduction: Advanced Solid-State Lasers 2020

Smart Energy 13 (2024) 100127

Contents lists available at ScienceDirect

Smart Energy

journal homepage: www.journals.elsevier.com/smart-energy

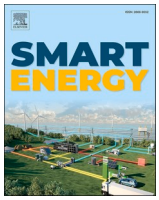

Trade-off between optimal design and operation in district cooling networks

Manfredi Neri *, Elisa Guelpa, Vittorio Verda

Department of Energy, Polytechnic University of Turin, Corso Duca Degli Abruzzi 24, 10129, Turin, Italy

ARTICLE INFO

Keywords:
District cooling
Thermal network
Genetic algorithms
Quadratic programming
Optimization

ABSTRACT

Especially in densely populated areas, district cooling represents an opportunity to reduce energy consumption and emissions. Nevertheless, this technology is characterised by large capital costs which impede its diffusion. As a consequence, optimization tools can significantly help to unleash their potential. In this paper, a methodology is proposed to combinedly optimize the design and operation of a district cooling system based on a Mixed Integer Quadratic Programming. The model is compared to the design only optimization, based on a properly tailored heuristic approach. The models, when applied to a case study characterized by seasonal demand, provide similar solutions, which differ by 0.5 % in terms of objective value for a standard scenario. The simultaneous design and operation optimization does not provide sensible savings with respect to optimizing solely the design. A sensitivity analysis is performed to prove the robustness of the results. The results showed that the simultaneous operation and design optimization would be limited to 1 % of total costs in the case of seasonal cooling demand. On the other hand, if the cooling demand persists throughout the year, as in tropical climates, the combined optimization provides significant benefits, since these savings reach 4.7 % of total costs.

1. Introduction

Building energy consumption accounts for 40 % of total demand and 36 % of CO2 emissions in Europe [1]. Over the last twenty years, building space cooling has more than tripled and is one of the most rapidly increasing energy end use sectors [2]. Moreover, it is expected that more than two thirds of buildings will have space cooling systems installed [3]. By 2050, the cooling demand of residential and commercial buildings is estimated to increase by up to 750 % and 275 %, respectively [4]. In 2019 the cooling sector was responsible for the emission of 1Gton of CO2. Moreover, the global yearly cooling demand is estimated to be 1900 TWh of electricity, accounting for the 16 % of building electricity consumption. Building space cooling is also responsible for high demand peaks during heat waves, which can cause blackouts or critical instabilities to the grid. As a consequence, with the increasing cooling demand, it is fundamental to invest and rely on more efficient technologies. District cooling is a suitable solution in areas with large energy density, such as central business districts or commercial areas [5], and more in general, buildings with higher cooling demand.

District cooling systems utilize central production units to supply chilled water to connected users through underground insulated pipes [6]. They are usually more efficient than individual cooling due to different reasons. First of all, in larger chillers the ratio between the cooling energy produced and the electricity required, known as energy efficiency ratio (EER), is larger with respect to smaller residential chillers. Moreover, the more homogeneous load curve and reduced peaks in district cooling systems allow the chillers to operate closer to their design conditions, maximizing performance [7]. Lastly, thanks to the integration with renewable energy sources, the efficiency can further increase, and the environmental impact can be minimized [8]. In some cases, free cooling from water basins, rivers, or aquifers can be harnessed, increasing the chillers EER [9,10]. In addition, district cooling can also be integrated with waste heat from industrial processes or Combined Cooling, Heat and Power plants (CCHP), enabling synergies with other energy systems [11,12].

On the other hand, district cooling systems are characterized by large capital costs, which limit their economic potential, although they can provide sensible reductions in terms of energy consumptions and CO2 emissions [13]. Compared with district heating, the temperature difference between supply and return lines is smaller, therefore larger mass flow rates are required to transfer the same amount of thermal power [9]. Consequently, larger pipes are necessary, causing a higher impact of

* Corresponding author.
E-mail address: manfredi.neri@polito.it (M. Neri).

https://doi.org/10.1016/j.segy.2023.100127
Received 27 July 2023; Received in revised form 3 November 2023; Accepted 18 November 2023
Available online 23 November 2023

piping and pumping costs on the total life-cycle expenditures [14]. Furthermore, the energy transfer stations in district cooling systems are more expensive, since due to the lower temperature difference, larger heat exchangers are required. Moreover, in Europe the heating season is much longer than the cooling one, hence the yearly savings are limited and have a smaller impact on the total life-cycle costs. However, with the increase of electricity cost, the interest in district cooling is rising, thanks to the potential increase of economic savings [15,16].

In this context, optimization tools represent an opportunity that may help to reduce the costs of district cooling systems and to exploit their full potential. Several authors have implemented models for the optimal design and operation of district cooling systems, including heuristic or mixed-integer linear programming models [17]. Powell et al. [18] implemented a dynamic programming model for the optimal operation of a district cooling system with thermal energy storages. The results showed that the model allows to reduce energy consumption by 9.4 % and operation expenditures up to 17.4 %. Wang et al. [19] developed a hybrid model that includes both data driven and physical modelling to describe the functioning of a district cooling system. The hybrid model was also coupled with a genetic algorithm to optimize chillers operation. The authors introduced variable search bounds in the constraints to limit the fluctuations of the variables that have a smaller impact on the optimization. Chiam et al. [20] developed a holistic framework for the optimal hourly operation of district cooling systems. The model is hierarchical, as it is characterised by a genetic algorithm at a master level, whose decision variables constitute the parameters for a MILP model at inferior level. They optimized simultaneously the flow and temperature variables, while respecting non linearities and managed to achieve reductions of emissions up to 31 %. Guelpa et al. [21] proposed a reduced order model for the simulation of district heating systems. They also coupled this model with a genetic algorithm to optimize the operation, minimizing the pumping costs. The reduced order model proved to be accurate, and the computational cost decreased by 80 % compared to physical models. The optimal strategy would allow to save up to 20 % of pumping costs with respect to conventional operating conditions. Cox et al. [22] implemented a model predictive control strategy based on artificial neural networks coupled with a genetic algorithm to optimize the operation of a district cooling system integrated with a thermal energy storage. The model implemented is able to reduce the operation expenditures up to 16 %. Nova-Rincon et al. [23] proposed a dynamic programming approach based on 2D orthogonal collocation for the operation optimization of district cooling systems. In particular, the objective was to select the mass flow rates in order to avoid the low ΔT syndrome. Yan et al. [24] proposed a multi-objective optimization framework based on a sequential least squares programming algorithm for the operation of district cooling systems. The objective was to minimize the thermal discomfort and the operation costs. Zhang et al. [25] developed a control logic for multi-cold source district cooling systems. Moreover, they compared the results in presence or absence of ice thermal storage. They showed that thanks to ice thermal storage, it is possible to save up to 6.7 % in terms of operating costs. Dominkovic et al. [26] evaluated the potential of district cooling in tropical climates under different scenarios, using the EnergyPlan optimization tool. The results suggested the use of waste heat by means of absorption chillers and the use of cold energy storages to balance the electricity surplus of intermittent renewable energy sources. Matak et al. [27] modelled the integration of a waste-to-energy incineration plant in a district heating and cooling system. The results showed that in the summer the thermal energy produced by the plant is 33 % higher compared to winter, making it particularly attractive for district cooling, especially if thermal storage is installed.

Concerning design optimization of district heating and cooling networks, different authors proposed heuristic or deterministic algorithms to select the optimal network layout, the pipe diameters, the buildings to be connected, or the capacity, number and position of production units and storages.

Regarding the optimization of chiller design, Ismaen et al. [28] developed a Mixed Integer Linear Programming model to optimize the capacities and operation of chillers in a district cooling system. The results showed that, in case of variable cooling demand, the optimal solution consists in selecting more chillers and storages of different sizes and capacities. In this way, the chillers would operate longer at design conditions with maximum efficiency. Alghool et al. [43] developed a Mixed Integer Linear Programming to optimize the design and the operation of a solar assisted district cooling system. They optimized the sizes of solar collectors, absorption and electrical chillers, the storage capacity and the annual hourly production schedule. The results showed that the solar collectors would provide 46 % of the thermal energy required by absorption chillers.

Different authors optimized the topology of district heating and cooling systems, focusing mainly on the layout and on the pipe diameters. Chan et al. [29] implemented a genetic algorithm integrated with a local search approach for the layout optimization of a district cooling network. In particular, they considered a graph in which every node is linked to all the other nodes and the problem of finding the optimal subtree network that minimizes both piping and pumping cost. Zeng et al. [30] developed a mathematical model to establish the annualized cost of a district heating and cooling network, based on the hourly load and optimized the pipe diameters through an integer encoded genetic algorithm. Egberts et al. [31] proposed a hybrid model characterised by a MINLP and a genetic algorithm for the optimization of the layout and pipe diameters of a district heating network. Moreover, the authors solved the problem guaranteeing robustness, taking into account the uncertainty of parameters such as demand or energy prices. Dobersek and Goricanec [32] optimized the network layout of a district heating system, minimizing capital and operation costs through a nonlinear algorithm. Al-Noaimi et al. [33] optimized the layout of a district cooling system through a MILP model based on an approximate decomposition, minimizing the sum of capital and operation costs. They considered an initial looped network with different locations for production units and storages. The objective of their model was to find the optimal tree-shaped subnetwork, the diameters and the location and size of storages and chillers, while the buildings connected to the network were known a priori. Dorfner et al. [34] developed a MILP model to optimize the layout and diameters of a district cooling network, considering the installation of redundant pipes in case of unavailability of some of the chiller plants. They applied the model to the Singapore district cooling network case study.

Other authors optimized the layout of district heating and cooling networks by means of heuristic approaches. Allen et al. [35,36] considered different case studies and demonstrated that the minimum spanning tree coincides with the optimal solution. Other authors suggested the use of the shortest path between the production unit and the users to select the topology of a thermal network [37,38].

Few authors optimized district cooling networks taking into account the non-linearity of pressure drops and pumping cost, which can reach 10 % of total operation expenditures, especially in larger networks. Moreover, a few authors optimized the set of users to be connected to a district heating and cooling network. Chow et al. [39] investigated on the optimal building mix that would be preferable to have in a district cooling system in order to have the demand curve as smooth as possible. The objective of the optimization was therefore to find the optimal mix of buildings that maximized the ratio between average and peak demand. Bordin et al. [40] instead, implemented a mathematical model to optimize the expansion of existing district heating networks. The goal of the algorithm was therefore to select the optimal set of new users that should be connected to the existing network maximizing the profits for the utility. However, this model does not take into account pumping costs, which in the case of district cooling can have an impact on the optimal solution. Neri et al. [41] implemented a MILP and a heuristic model to optimize the layout and the set of users to be connected to district cooling networks, minimizing the sum of capital and operation

costs and taking into account the non-linearity of pressure drops and pumping costs. The MILP model proved to be more accurate than the heuristic, but the latter is more than 90 % more efficient, while the solution differs about 1% from the one obtained by the MILP. However, the models are limited only to single plant district cooling system and thermal energy storage options are not considered. Dominkovic and Krajacic [42] implemented a linear programming model to determine the optimal share of district cooling in an urban context and the optimal size of thermal storage in different scenarios, minimizing the total socio-economic costs. They found that in the case of Singapore, the optimal solution consists in satisfying 30 % of cooling demand with district cooling and the other 70 % with individual cooling solutions.

The optimal position of production plants in district heating and cooling networks has been addressed by few authors. Guelpa et al. [44] developed a genetic algorithm to optimize the location of heat pumps in a district cooling system to minimize the sum of capital and pumping costs. Wang et al. [45] optimized the position of a peak load boiler in a district heating network, showing that it should be placed in areas with high load density. Khir and Haouari [46] implemented Mixed Integer Programming models to optimize the network layout, the pipe diameters, the daily production schedule and the position and capacity of chillers and storages in a district cooling system.

From the literature analysis, it emerges that when optimizing the design of district cooling networks, most authors focus on one or few specific aspects, such as the layout, the pipe diameters, the buildings to be connected or the position of the plants. There is hence a clear research gap in literature, as no author addressed the problem of simultaneously optimizing the buildings to connect to a thermal network and the position of the production units. Indeed, the potential of district cooling systems is highly dependent on both factors. The position of centralized chillers and storages influences the piping and pumping costs, while the set of buildings to be connected to a district cooling system has an impact on the capital and operation expenditures. Moreover, the economic feasibility of connecting a building to a district cooling network depends on the position of the chiller plants. As a consequence, optimizing both aspects can lead to a major reduction of total costs and a higher penetration of district cooling in a defined urban context. However, simultaneously optimizing all the parameters is not trivial, as computational cost is larger, especially if the non-linearity of pressure drops and pumping power is taken into account.

In this paper, the simultaneous design and operation optimization has been implemented and compared to a design only optimization. The design optimization is done by an innovative iterative genetic algorithm with the number of variables progressively increased, which allows keeping the number of variables low. By using this approach, the model starts optimizing the problem with less decision variables, finding an initial coarser solution, which is then updated at each iteration, by optimizing the problem with an increasing number of variables. The combined optimization is done using a Mixed Integer Quadratic Constrained Programming (MIQCP) model that optimizes both the design and the operation schedule of a district cooling network with thermal energy storage. The objective of this model is to find a trade-off between the minimization of capital and operational expenditures. Lastly, the two models are compared by applying them to a case study (analysed in different scenarios) and to show the differences between optimizing only the design and optimizing both design and operation. A sensitivity analysis was also conducted to determine the impact of electricity tariff and chiller cost on the trade-off between design and operation optimization.

The main research gaps of the analysis are: 1) show the optimization of either the operation and the design of district heating and cooling systems 2) propose a novel approach to keep low computational costs for design optimization (this opens the possibility to use it for multi-scenario analyses) 3) show which are the benefits provided by the combined design and operation optimization, instead of design only optimization, for different scenarios.

2. Design optimization

The goal of this model is to optimize the design of a district cooling network minimizing the sum of capital and operation expenditures. In particular, the model through a genetic algorithm optimizes the set of users that shall be connected and the position of chillers and storages. The model is based on the following assumptions.

- The network is tree-shaped.
- Thermal losses are neglected, hence the temperature is homogenous on both supply and return lines.
- The cooling power production of every chiller is constant and storages are used for peak shaving and valley filling.
- The demand of each building is always satisfied by the same chiller. This assumption is based on the fact that, in order to minimize pumping costs, the cooling demand of buildings should be satisfied by chiller plants close to them.
- Every chiller relies on a specific storage, hence the extra/deficit production is absorbed/released always by the same storage).

The operation is therefore not optimized in this model, since it is assumed that the chillers operate at constant load and that the storages are sized accordingly.

The model is characterized by two types of integer decision variables: x_i and x_j. The variable x_i indicates whether the generic user i is connected or not to the network and by which chiller is fed. It can range between zero and the number of possible chiller locations. If it is equal to zero, the user i is not connected to the network, while if it is equal to j, it is connected and fed by the chiller indexed with j. Similarly, the variable x_j indicates on which storage the generic chiller j relies on. Table 1 summarizes how these variables are encoded. The other variables, such as the size of chillers and storages, the mass flow rate flowing in every branch of the network, the cooling power production and the cooling energy absorbed or released by the storage, are all dependent on x_i and x_j and are evaluated simultaneously with the cost function. The nomenclature for indices, the sets and the parameters is defined in Tables 2 and 3, while in Table 4 are shown the values of the main parameters used for the optimizations. The costs for different sizes of energy transfer stations are reported in Table 5.

2.1. Cost function

The cost function is the sum of capital and operation expenditures, as shown by Eq (1):

$$cost_{tot} = cost_{chillers} + cost_{op,chillers} + cost_{piping} + cost_{pumping} + cost_{ETS} + cost_{storage} \quad (1)$$

where.

- $cost_{chillers}$ is the capital cost for the installation of chillers;
- $cost_{op,chillers}$ is the operation cost of chillers;
- $cost_{piping}$ is the capital cost of piping;
- $cost_{ETS}$ is the capital cost for the installation of energy transfer stations;
- $cost_{storage}$ is the capital cost for storage installation.

The objective is therefore to minimize the total life-cycle costs. The

Table 1
Encoding of model variables.

Variable value	Meaning
$x_i = 0$	Building i not connected
$x_i = j$	Demand of building i is fed by chiller j
$x_j = k$	Chiller j is connected to storage k

Table 2
Sets and indices defined in both models.

Set/Index	Description
Ut	Set of users
Ch	Set of chillers
St	Set of Storages
V	Set of intermediate nodes
H	Set of pipe diameters
B	Set of network branches
T	Set of time instants
i	Index referring to the generic user
j	Index referring to the generic chiller
k	Index referring to the generic storage
l	Index referring to the generic branch
v	Index referring to the generic intermediate node
t	Index referring to the generic time instant

Table 3
Parameters used in both models.

Parameter	Description
EER_{DC}	EER of large-scale chiller in district cooling networks
EER_{ind}	EER for small scale chillers in individual cooling systems
$G^t_{ext,i}$	Mass flow rate requested by generic user i at time t [kg/s]
L_l	Length of branch l [m]
c^t_{el}	Cost of electricity at time t [€/kWh]
$c_{chill,DC}$	Cost of centralized chiller per unit of size [€/kW]
$c_{chill,ind}$	Cost of individual chiller per unit of size [€/kW]
$c_{storage}$	Cost of storage per unit of size [€/kWh]
$c_{ETS,i}$	Cost of energy transfer station installed at user i [€]
c^h_{pipe}	Cost of pipe with diameter h per unit of length [€/m]
ΔT	Temperature difference between supply and return [K]
c_p	Specific heat [kJ/(kJ*K)]
n_d	Duration of cooling season [days]
n_y	Life cycle of the system [years]
r	Discount rate [%]
Δt	Time interval between two steps [s]
N	Number of time instants
$max\ G^h$	Maximum mass flow rate admissible for a pipe with diameter h [kg/s]
$min\ G^h$	Lower bound of the maximum mass flow rate for a pipe with diameter h [kg/s]
η_{charge}	Charge efficiency of thermal energy storage [%]
$\eta_{discharge}$	Discharge efficiency of thermal energy storage [%]
A	Incidence matrix

Table 4
Values of main parameters.

Parameter	Value
EER_{DC}	6.5 [47]
EER_{ind}	2.7 [47]
$c_{storage}$	20 €/kWh [48]
$c_{chill,DC}$	400 €/kW [47]
$c_{chill,ind}$	600 €/kW [47]
n_y	30 y
n_d	60 d
r	5%
ΔT	7 °C
η_{pump}	80 % [49]
η_{charge}	95 %
$\eta_{discharge}$	95 %
N	24
Δt	1 h

Table 5
Cost of energy transfer stations [47].

Size [kW]	10	100	200	300	500	1000
Cost [k€]	5.4	44	55	65	79	108

capital costs represent the initial investments, while the operation costs are the sum of total operation expenditures during the lifetime of the system, adjusted by an actualization coefficient, which depends on the lifetime of the system and on the discount rate. This allows to evaluate the present value of future expenditures.

2.1.1. Capital cost of energy transfer stations

The size and the cost of energy transfer stations depend on the demand peak of the single buildings, whose demand profile are an input of the model, hence they are known a priori. The only unknown is whether a building is connected to the network or not. Hence, the capital cost of energy transfer stations can be defined as:

$$cost_{ETS} = \sum_{i|x_i>0}^{Ut} c_{ETS,i} \tag{2}$$

where $c_{ETS,i}$ is the cost of the energy transfer station of building i. The condition $i|x_i > 0$ indicates that only buildings connected to the district cooling network are taken into account.

2.1.2. Capital cost of chillers and storages

The capital cost of chillers and storages is proportional to their sizes. Concerning the chillers, the model provides two options: individual chillers characterized by larger cost per unit of size and centralized chillers characterized by lower cost per unit of size. The total capital expenditure for chillers is therefore defined as:

$$cost_{chillers} = \sum_{j}^{Ch} c_{chill,DC} * S_j + \sum_{i|x_i=0}^{Ut} c_{chill,ind} * S_i \tag{3}$$

where the first term refers to the cost of centralized chillers and the second term refers to the cost of individual chillers. The condition $i|x_i = 0$ indicates that only buildings not connected to the network, hence with an individual cooling system, are taken into account. S_j is the size of the generic centralized chiller indexed with j, while S_i refers to the size of the independent chiller of the generic user indexed with i. The size of individual chillers is known a priori, since it depends only on the demand peak, which is an input of the model. On the other hand, the size of centralized chillers depends on the variables x_i and x_j, since it was assumed that every user is fed by only one chiller and that every chiller operates at constant power. The mass flow rate inserted from a generic chiller into the network is evaluated as:

$$G^t_{ext,j} = -\frac{1}{\mathrm{N}} \sum_{t}^{T} \sum_{i|x_i=j}^{Ut} G^t_{ext,i} + Losses \quad \forall j \in Ch \tag{4}$$

where N is the number of time steps and $G^t_{ext,i}$ is the mass flow rate of chilled water requested by the generic user i at time t. The condition $i|x_i = j$ indicates that only the users fed by chiller j are considered. The *Losses* term refers to the additional mass flow rate that the chillers should introduce in order to compensate the heat losses of thermal energy storages. This term is calculated by computing the theoretical mass flow rate inserted from the chillers and that would be absorbed by the thermal energy storages in the ideal case of unitary efficiency and multiplying it by a loss factor, which itself is evaluated as:

$$L_f = 1 - \eta_{charge} * \eta_{discharge} \tag{5}$$

where η_{charge} and $\eta_{discharge}$ are the thermal energy storage efficiencies during charge and discharge. The mass flow rates absorbed or released by the thermal energy storages are evaluated as stated in Eq. (6):

$$G^t_{ext,k} = \sum_{j|x_j=k}^{Ch} \left(G^t_{ext,j} + \sum_{i|x_i=j}^{Ut} G^t_{ext,i} \right) \quad \forall\, k \in St \tag{6}$$

where $G^t_{ext,k}$ is the generic mass flow rate absorbed/released by the

generic storage indexed with k at time t. The term in parentheses is the extra/deficit mass flow rate that every chiller inserts in the network with respect to the users' demand. The condition $j|x_j = k$ indicates that only the chillers connected to the k storage are taken into account, as for hypothesis it was assumed that the extra/deficit mass flow rate of every chiller is always absorbed/released by the same storage. Once the mass flow rates are evaluated, the sizes of chillers and storages can be easily determined and consequently their cost. The size of the generic chiller is therefore given by the cooling power that it has to produce, which is equal for all time instances, as hypothesized.

$$S_j = G^t_{ext,j} * c_p * \Delta T \quad \forall j \in Ch \tag{7}$$

where c_p is the specific heat and ΔT is the temperature difference between supply and return pipes. The sizes of the storages depend on the cumulate function of the cooling energy absorbed/released. In particular, they are equal to the difference between the maximum and the minimum of this function. In fact, this value indicates the minimum size that a storage must have to be able to satisfy the demand.

$$\begin{aligned} S_k = &max \sum_{t=0}^{t} G^t_{ext,k} * c_p * \Delta T * \Delta t \\ &-min \sum_{t=0}^{t} G^t_{ext,k} * c_p * \Delta T * \Delta t \quad \forall k \in St \end{aligned} \tag{8}$$

The capital cost of storages can be then computed as defined in Eq. (9):

$$cost_{storage} = \sum_{k}^{St} S_k * c_{storage} \tag{9}$$

2.1.3. Chillers operation costs

The operation costs of the chillers are equal to the actualized operation expenditures of the chillers, which depend on the yearly electricity consumption, the electricity cost and the lifetime of the system. The yearly electricity consumption depends on the EER of the chillers, on the cooling demand and on the duration of the cooling season. As a consequence, the electricity consumption is evaluated considering a reference day and it is multiplied by the number of utilization days of the system within a year. This assumption is justified by the fact that the daily demand profile tends to be cyclic, as it depends especially on the use of the cooling systems, which itself depends on other factors like working hours and daily routines. On the other hand, the daily peaks vary and depend on the climate conditions. The shape of the demand curve has a certain pattern that depends on the type of building and on the users' routines, while the amplitude of the curve depends mostly on the climate conditions. Consequently, it is sensate to compute the yearly consumption using a typical reference day and the number of usage days. The EER depends on the type of chillers. Two possible types have been considered: centralized ones with better performances and individual ones with lower performances. Eq. (10) defines the operation costs of centralized chillers:

$$\begin{aligned} cost_{op,chillers-DC} = &\sum_{t}^{T} \sum_{j}^{Ch} \left(\frac{G^t_{ext,j} * c_p * \Delta T * \Delta t}{EER_{DC}} * c^t_{el} \right) \\ &* n_d * \sum_{n=1}^{n_y} \frac{1}{(1+r)^n} \end{aligned} \tag{10}$$

where r is the discount rate, n_y is the chiller lifecycle in years, n_d is the length of cooling season expressed in days. The first fraction is the ratio between the cooling energy produced in the generic time interval and the energy efficiency ratio. Consequently, it represents the electrical energy required during the generic time interval by the chiller j. By multiplying this fraction for the cost of electricity, the electricity expenditure of the chiller j over the time interval t is obtained. The daily operation expenditures of centralized chillers are given by summing over all chillers and time intervals. By multiplying the daily expenditures for the length of the cooling season n_d, the yearly electricity expenditure of centralized chillers is obtained. Lastly, the actualized operation costs are given by multiplying the yearly operation costs for the actualization factor, which is represented by the last summation term. This factor actualizes the expenses that are not faced immediately. Similarly, the operation cost of individual chillers is defined in Eq. (11).

$$\begin{aligned} cost_{op,chillers-ind} = &\sum_{t}^{T} \sum_{i|x_i=0}^{Ut} \left(\frac{G^t_{ext,i} * c_p * \Delta T * \Delta t}{EER_{ind}} * c^t_{el} \right) \\ &* n_d * \sum_{n=1}^{n_y} \frac{1}{(1+r)^n} \end{aligned} \tag{11}$$

where $G^t_{ext,i}$ is the mass flow rate requested by user i at time t. The operation costs of centralized and individual chillers therefore differ, due to the different values of EER. In the case of centralized ones, the EER is generally higher. The total chillers operation cost is defined as:

$$cost_{op,chillers} = cost_{op,chillers-DC} + cost_{op,chillers-ind} \tag{12}$$

2.1.4. Piping cost

In order to evaluate the piping cost, it is necessary to compute first the mass flow rates in every branch of the network. Once the mass flow rates entering or exiting from each node are evaluated, the mass flow rate in every branch can be computed by solving the continuity equation in every node, which in matrix form is expressed as the following linear system:

$$A * G^t + G^t_{ext} = 0 \tag{13}$$

where A is the incidence matrix, G^t is the vector that includes the mass flow rates in every branch of the network at time t and G^t_{ext} is the vector of entering/exiting mass flow rates in each node at time t. An incidence matrix expresses the relation between nodes and edges of a graph. If the node i is an entry node of the edge j, the element a_{ij} of the matrix is equal to 1, while it is equal to -1 if i is an exit node. If i is neither an entry nor an exit, the element a_{ij} is null. The diameters are chosen so that the maximum velocity does not exceed 1.5 m/s. For each pipe it is therefore selected the smallest diameter that can satisfy this constraint. The piping cost can then be evaluated as:

$$cost_{piping} = \sum_{l}^{B} \sum_{h}^{H} L_l * x^h_l * c^h_{pipe} \tag{14}$$

where L_l is the length of the branch l, x^h_l is an auxiliary binary variable that indicates whether the diameter h is selected for the branch l and $c_{pipe}{}^h$ is the cost per unit of length for a pipe with diameter h.

2.1.5. Pumping cost

After the mass flow rates and the pipe diameters have been evaluated, the pressure drops and pumping costs can be computed. The pressure drop at the generic time instant along the generic pipe is calculated as defined in Eq. (15).

$$\Delta p^t_l = 8 * \frac{\left(f * \frac{L_l}{D_l} + \beta_l \right) * G^{t\,2}_l}{\rho * {D_l}^4 * \pi^2} + \rho * g * \Delta z_l \tag{15}$$

Where.

- ρ is the density;
- f is the friction coefficient;
- D_l is the diameter of the pipe l;
- β_l is the sum of the coefficients of localized pressure drops;
- $G_l(t)$ is the mass flow rate flowing in pipe l at time t;
- g is the gravitational acceleration;

- Δz_l is the height difference between the exit and entry node of the pipe l;
- $\Delta p_l(t)$ is the pressure drop on the pipe l at time t.

It is hypothesized that the pumping stations are located in the same positions of the chillers and storages, hence in all the nodes in which mass flow rate enters into the network. The mechanical power provided by the pumps is therefore calculated as defined in Eq. (16):

$$P^t_{pump,mech} = \sum_{in}^{Ch\cup St} \frac{G^t_{ext,in} * \Delta p^t_{in}}{\rho} \tag{16}$$

Where the index *in* refers to the generic chiller or storage node from which a mass flow rate is inserted into the network, Δp^t_{in} is the pressure increase due to the presence of a pump and η_{pump} is the efficiency of the pump. The electric power required by the pumps instead is computed by dividing the mechanical power with the efficiency of the pumps.

$$P^t_{pump,el} = \frac{P^t_{pump,mech}}{\eta_{pump}} \tag{17}$$

The pumping cost is then evaluated multiplying the energy consumed by the pumps in each time interval by the cost of electricity, as defined in Eq. (18):

$$cost_{pumping} = \sum_{t}^{T} P^t_{pump,el} * \Delta t * c^t_{el} * n_d * \sum_{n=1}^{n_y} 1 \Big/ (1+r)^n \tag{18}$$

2.2. Clustering approach

The complexity and the computational cost of the model depends on the number of variables. In the case of a network with a large number of users, the problem may become too complex and it may be difficult for a genetic algorithm to converge to the global optimum. As a consequence, a clustering approach has been implemented in order to reduce the number of variables of the problem. This approach consists in grouping the users in clusters based on their distance on the graph. A unique decision is taken for all the users part of the same clusters, since it is highly probable that users close to each other should be either fed by the same chiller or all disconnected from the network. The algorithm implemented to group the users in clusters is called "k-minimum spanning tree" [50] and is formed by the following steps.

- Find the minimum spanning tree of the network if it presents any loops.
- Delete the k-1 branches.
- Extract the k subnetworks that formed.

These k subnetworks represent the clusters and the nodes part of the same subnetwork are all part of the same cluster. In Fig. 1 is shown schematically how the algorithm works for a simple graph.

2.3. Iterative procedure

The clustering approach allows to solve the problem with a lower number of variables, easing the convergence to the optimum. However, if the number of clusters is too small and its users are far from each other, the solution may differ from the optimal one. On the other hand, if a large number of clusters is chosen, the algorithm may struggle to converge, or it may converge to a local optimum. As a consequence, an iterative approach has been implemented, which consists in solving the problem with an increasing number of clusters [41]. At each iteration a genetic algorithm is used to solve the problem, using the previous known solution as a member of the initial population. This method, hence,

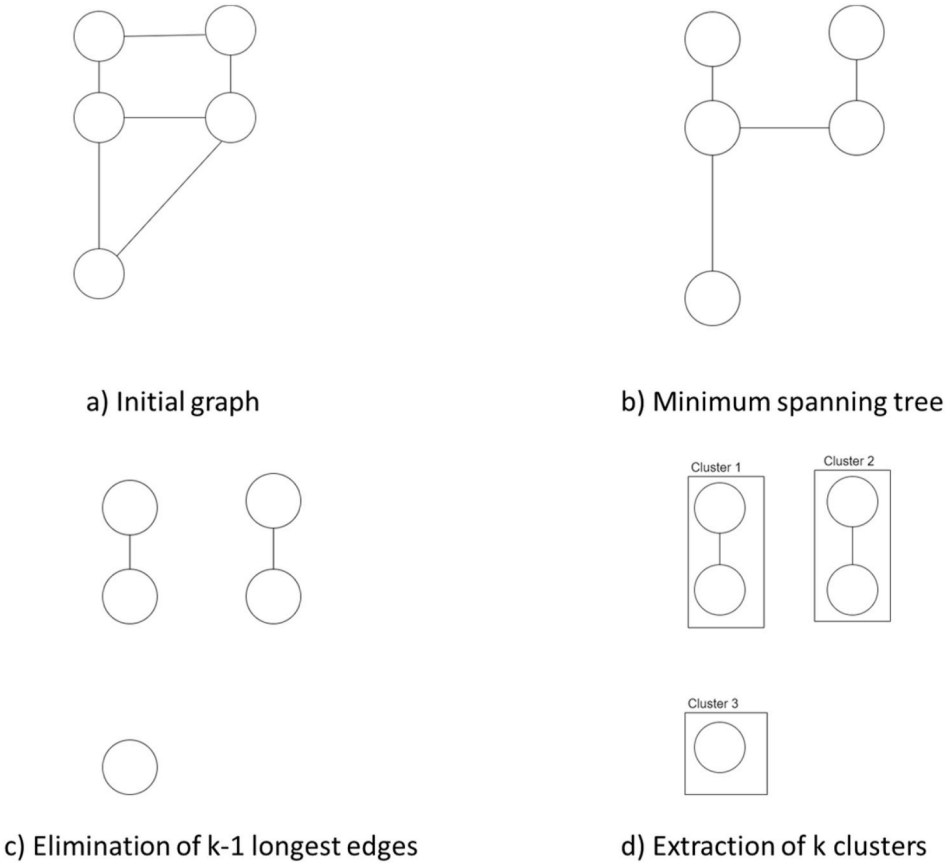

Fig. 1. k-minimum spanning tree algorithm with k = 3.

exploits the knowledge of a coarser optimal solution, obtained with a lower number of variables and looks for a more accurate one in its neighborhood, introducing additional variables. The procedure starts with a sufficiently low number of clusters and at each step, a cluster is divided in two new clusters. The iterations are stopped when the pre-fixed number of clusters is reached.

3. Design and operation optimization

This model has the objective of minimizing the sum of operation and capital expenditures of a district cooling network. Differently from the heuristic model previously explained, the set of users to be connected is an input of the problem and this is not optimized. On the other hand, the scheduling of the chillers and storages is optimized simultaneously with the design of the system. The model is nonlinear and non-convex and has been formulated using the paradigm of Mixed Integer Quadratic Constrained Programming (MIQCP) and has been solved using Gurobi [51]. The reason for which it was chosen a nonlinear non-convex model is linked to the presence of bi-linear constraints, whose linearization is complex to handle. Table 6 defines the variables of the model, while the sets, indices and the parameters are the same already defined for the heuristic model in Tables 2 and 3

3.1. Cost function

The cost function is the sum of capital and operation costs. In this case, the users are all connected to the network, because the number of users is already known, therefore the cost of chillers for buildings not connected to the network is not considered. Moreover, the cost for energy transfer stations is fixed for the same reason and does not depend on the decision variables. The other terms of the cost function are defined as in the previous model.

3.2. Constraints

The model is characterized by linear and nonlinear constraints, which are defined in the following paragraphs.

3.2.1. Mass balance constraints

The following constraints ensure that mass balance is respected for every type of node. Eq. (19) is the mass balance applied to the chiller nodes at a generic time instant.

$$\sum_{l\in B} a_{j,l} * G_l^t + G_{ext,j}^t = 0 \quad \forall\, j \in Ch, t \in T \tag{19}$$

Table 6
List of model variables.

S_j	Size of generic chiller j
S_k	Size of generic storage k
x_l^h	Binary variable equal to 1 if the diameter h is selected for pipe l
G_l^t	Mass flow rate flowing in pipe l at time t
$G_{ext,j}^t$	Mass flow rate entering from chiller j at time t into the network
$G_{ext,k}^{t+}$	Mass flow rate absorbed from storage k at time t
$G_{ext,k}^{t-}$	Mass flow rate released from storage k at time t
C_k^t	Capacity of the storage k at time t
R_l	Fluid dynamic resistance of pipe l per unit of mass flow rate
p_s^t	Pressure on generic node s at time t
Δp_l^t	Pressure drop on pipe l at time t
$Gabs_l^t$	Absolute value of G_l^t
P_j^t	Pumping power required by pump at chiller node j and time t
Pk^t	Pumping power required by pump at storage node k and time t
$G2_l{}^t$	Product between G_l^t and its absolute value
$Gmax_l$	Maximum mass flow rate flowing in pipe l
yG_l^t	Binary variable that is equal to 1 if the maximum mass flow rate in pipe l occurs at time t, otherwise it is equal to 0

Where $a_{j,l}$ is the element on the j^{th} row and l^{th} column of the incidence matrix A. Eq. (20) reports the mass balance applied to the storage nodes at a generic time instant. The variable $G_{ext,k}^{t+}$ represents the mass flow rate absorbed by a storage at time t, while $G_{ext,k}^{t-}$ is the mass flow rate released at time t. The first variable is positive, while the second is negative, as the convention is that the mass flow rate exiting from the network has positive sign, while negative if it is entering in the network.

$$\sum_{l\in B} a_{k,l} * G_l^t + G_{ext,k}^{t+} + G_{ext,k}^{t-} = 0 \quad \forall\, k \in St, t \in T \tag{20}$$

Eq. (21) represents the mass balance applied to the user nodes at a generic time instant. In this case, the mass flow rate exiting from the network is known, since it depends on the demand of the users.

$$\sum_{l\in B} a_{i,l} * G_l^t = -G_{ext,i}^t \quad \forall\, i \in Ut, t \in T \tag{21}$$

Eq. (22) is the mass balance applied to a generic intermediate node v at a generic time instant t. These nodes are characterised by null external mass flow rates.

$$\sum_{l\in B} a_{v,l} * G_l^t = 0 \quad \forall\, \nu \notin Ut \cup Ch \cup St, t \in T \tag{22}$$

Constraint in Eq. (23) is a balance on the thermal energy storage, linking its variation of residual capacity with the mass flow rates entering or exiting from it, taking into account the thermal storage efficiency for charge and discharge.

$$C_k^t - C_k^{t-1} - G_{ext,k}^{t+} * cp * \Delta T * \Delta t * \eta_{charge} - \frac{G_{ext,k}^{t-} * cp * \Delta T * \Delta t}{\eta_{discharge}} = 0 \quad \forall k \in St, t \in T \tag{23}$$

Moreover, the additional constraint in Eq. (24) is added in order to impose a daily cycle of charge/discharge.

$$C_k^0 - C_k^N - G_{ext,k}^{0+} * cp * \Delta T * \Delta t * \eta_{charge} - \frac{G_{ext,k}^{0-} * cp * \Delta T * \Delta t}{\eta_{discharge}} = 0 \quad \forall\, k \in St \tag{24}$$

where the superscripts 0 and N refer to the first and last time steps.

3.2.2. Capacity constraints

The constraint in Eq. (25) ensures that the cooling power produced by a chiller is not greater than its capacity.

$$G_{ext,j}^t * cp * \Delta T \le S_j \quad \forall\, t \in T, j \in Ch \tag{25}$$

Constraint in Eq. (26) instead ensures that the maximum storage capacity is not exceeded.

$$C_k^t \le S_k \quad \forall k \in St, t \in T \tag{26}$$

3.2.3. Pressure constraints

Constraint in Eq. (27) defines the pressure drop in a generic pipe. Since the pressure drop depends on the square of mass flow rate, a new variable called $G2_l^t$ is introduced to represent the product between mass flow rate and its absolute value. This is different than the square of mass flow rate, which is always positive, since in this case the pressure drop and the mass flow rate must have the same sign.

$$\Delta p_l^t - G2_l^t * \sum_{h\in H} x_l^h * R_l^h = 0 \quad \forall\, t \in T, l \in B \tag{27}$$

Constraint in Eq. (28) links the pressure at the inlet and outlet of each pipe with its pressure drop. The indices l_{in} and l_{out} indicate the input and outlet nodes of the generic pipe indexed by l.

$$p_{l_{in}}^t - p_{l_{out}}^t - \Delta p_l^t = 0 \quad \forall\, t \in T, l \in B \tag{28}$$

Constraint in Eq. (29) guarantees that the pressure at user nodes is

larger than a minimum value.

$$p_i^t \geq p_{min} \quad \forall\, i \in Ut, t \in T \tag{29}$$

The bilinear constraints in Eqs. (30) and (31) define the variables P_j^t and P_k^t, which represent the electrical power required by the pumps located in chillers and storage nodes.

$$P_j^t + G_{ext,j}^t * \frac{p_j^t}{(\rho * \eta_{pump})} = 0 \quad \forall\, j \in Ch, t \in T \tag{30}$$

$$P_k^t + G_{ext,k}^{t-} * \frac{p_k^t}{(\rho * \eta_{pump})} = 0 \quad \forall\, k \in St, t \in T \tag{31}$$

Constraint in Eq. (32) defines the variable $G2_l^t$ as the product between the mass flow rate flowing in branch l at time t and its absolute value.

$$G2_l^t - Gabs_l^t * G_l^t = 0 \quad \forall\, l \in B, t \in T \tag{32}$$

Absolute value is not a linear function; therefore it is linearized by introducing the constraints in Eqs. (33) and (34), which ensure that the variable $Gabs_l^t$ is equal to the absolute value of G_l^t.

$$-Gabs_l^t + G_l^t \leq 0 \quad \forall\, l \in B, t \in T \tag{33}$$

$$Gabs_l^t + G_l^t \geq 0 \quad \forall\, l \in B, t \in T \tag{34}$$

3.2.4. Topology constraints

Constraint (35) guarantees that only one diameter is selected for each pipe.

$$\sum_h^H x_l^h = 1 \quad \forall l \in B \tag{35}$$

Constraints (36) and (37) restrict the maximum mass flow rate in each pipe to a defined range.

$$Gmax_l - \sum_h^H x_l^h * max\ G^h \leq 0 \quad \forall\, l \in B \tag{36}$$

$$Gmax_l - \sum_h^H x_l^h * min\ G^h \geq 0 \quad \forall\, l \in B \tag{37}$$

Constraints (38) and (39) ensure that the variable $Gmax_l$ is equal to the maximum mass flow rate in branch l. These auxiliary constraints therefore linearize the max function, introducing additional binary variables. The first constraint is a big-M constraint, where M is a constant whose value is larger than the upper bound of $Gmax_l$. Consequently, if the maximum occurs at t, yG_l^t is equal to zero and in order to satisfy both constraints, $Gmax_l$ must be equal to $Gabs_l^t$. If the maximum occurs at another instant different than t, the first constraint is satisfied only if yG_l^t is equal to one.

$$Gmax_l - yG_l^t * M - Gabs_l^t \leq 0 \quad \forall\, l \in B, t \in T \tag{38}$$

$$Gabs_l^t - Gmax_l \leq 0 \quad \forall\, l \in B, t \in T \tag{39}$$

4. Case study

Both models have been applied to the same case study. It was considered the topology of a distribution network of a Northern Italy district heating system, shown in Fig. 2. The area is characterized by 108 users, while three possible positions for chillers and six for storage are considered. Each building has a different volume, as represented by the radius of the green dots in the figure. The height difference is close to zero, hence the gravitational component was neglected in the pressure calculations.

The motivation for this choice of case study is related to the fact that this area is well-representative of a residential district in Mediterranean areas. As a consequence, although this is the topology of a district heating network, it constitutes a realistic case study for the application of district cooling in Mediterranean areas. Moreover, the district heating topology follows the shape that a district cooling would have, since it is built respecting typical urban constraints, such as the presence of buildings, roads, underground stations or water and gas piping systems.

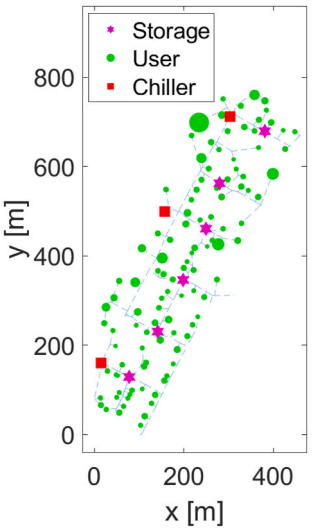

Fig. 2. Case study topology.

The cooling demand of every user has been calculated for a typical summer day using a dynamic model, described in the norm UNI EN ISO 52016–1 [52], whose inputs are only the building volumes and the weather data. The model handles the uncertainty of the thermophysical properties through stochastic distributions. The electricity cost was extracted by the historical archive of the Italian electricity market. In particular, it was considered the monthly average of the day-ahead market for January 2022 [53]. Both cooling demand and electricity cost profiles are shown in Fig. 3. It can be observed that the demand is larger in the time interval between 10 a.m. and 8 p.m., reaching a peak demand of about 7 MW. The electricity cost presents two peaks at 8 a.m. and 7 p.m. During the night, the cooling demand is null since HVAC systems are mainly operated during the day in the warmest hours. However, also electricity cost is low, reaching a minimum at 5 a.m., due to the lower electricity demand during the night. These profiles suggest the possibility to implement power-to-cool strategies. In particular, chillers could operate at higher load during the night, when electricity is cheaper and the demand is low. The cooling energy could be therefore stored and released when the electricity is expensive and demand is larger. This strategy has a limit, which depends on the size of chillers and pipes. In fact, if only operation costs are considered, the optimal solution would be to produce the whole daily cooling demand when the electricity cost is minimum. However, this solution would require extremely

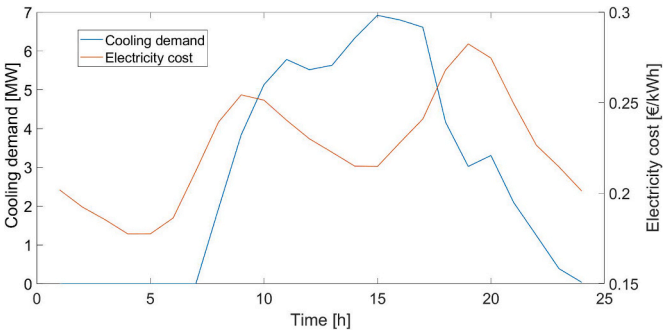

Fig. 3. Daily profiles of cooling demand and electricity cost.

large components and the capital costs would be too large. Conversely, if only capital costs are minimized, the solution would consist in a constant cooling production, since in this way the size of chillers and pipes would be minimum. On the other hand, the operation schedule in this solution would not be optimal. As a consequence, one of the goals of this study is to determine if there is a trade-off between the two solutions. The objective is therefore to verify if it is beneficial installing larger chillers and pipes in order to be able to have a better operation schedule and obtain major savings. This problem was defined through the model for operation and design optimization (MIQCP, section 3). The model for the design optimization (heuristic, section 2), instead optimizes the set of users to be connected to a district cooling network and the position of chillers and storages.

5. Results

In this section are presented the results obtained by both optimization models. The simulations have been carried out on a laptop with the CPU Intel Core i7-510 1.8 GHz.

5.1. Design optimization

The maximum number of clusters was fixed to 20 and the model took 25 min to find the optimal solution, which is shown in Fig. 4.

According to the solution, 104 out of 108 users should be connected to the district cooling network and three chillers should be installed, each connected to a different storage. Fig. 5 shows the different costs of the optimal network. It can be observed that the capital costs are dominant and account for 73 % of the total expenditures. In particular, the capital costs for piping and energy transfer stations are the highest ones, representing the 24 % and 32 % of total costs, respectively. Concerning operation expenditures, chillers operation cost is the main one. However, pumping is not negligible and accounts for about 11 % of total operation expenditures.

5.2. Design and operation optimization

The optimal set of users and the network layout found with the heuristic algorithm has been considered as an input for the MIQCP model. The demand profile is therefore known, while the sizes of chillers and storages need to be optimized, as well as their scheduling. The optimization was launched and run for three days, but did not converge to the global optimum. However, it found a solution with an optimality gap of 2 %, which means that the local optimum found is, to the utmost,

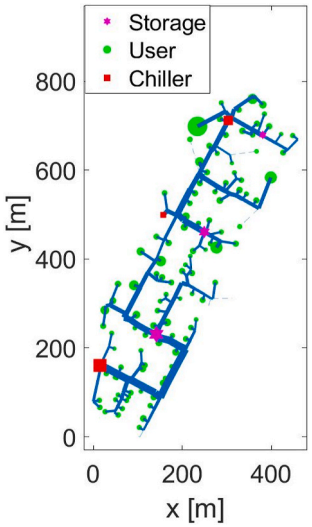

Fig. 4. Optimal network design according to design optimization model.

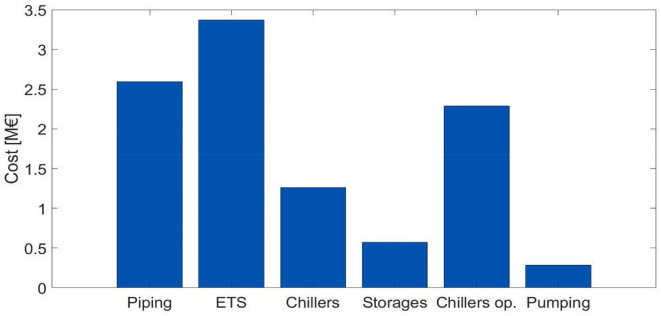

Fig. 5. Cost details of optimal district cooling network achieved with design optimization.

2 % more expensive than the global one. The large computational cost and the difficulty to converge is due to the large number of variables and the bilinear constraints, which not only are non-linear, but also they cause the non-convexity of the problem. In Fig. 6 it is shown the resulting optimal network layout. The sizes of chillers and storages are slightly different from the ones obtained with the design optimization model. In fact, the total storage and chiller capacity is almost the same, but it is distributed differently in the two solutions. This is also summarized in Table 7.

In Fig. 7 it is shown the optimal hourly scheduling for chillers and storages. It can be observed that the cooling production by the chillers is almost constant during the day, since the ratio between the average and the peak load is 98 %. The storages are therefore used mainly for peak shaving and valley filling. They, in fact, store the extra cooling energy produced during the night and to release it when production of chillers alone can not satisfy the demand.

Fig. 8 shows the cost details of this solution and the comparison with the design optimization solution. With respect to the solely design optimization, the costs are only 0.5 % lower. The results therefore are almost equal for the two solutions obtained with the different models.

6. Sensitivity analysis

The previous results show that for this case study it is possible to design and size district cooling networks considering a constant cooling

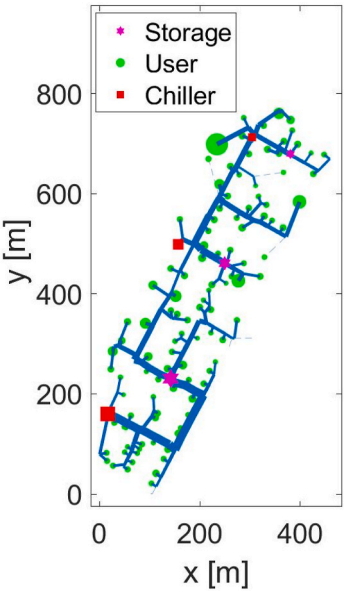

Fig. 6. Optimal district cooling topology according to the operation and design optimization.

Table 7
Chiller and storage sizes.

Chiller/storage coordinates (x, y)	Size (Operation and design opt)	Size (Design opt.)
(380.8374,679.2562)	4.9 MWh	5.1 MWh
(141.6696,230.7191)	14.5 MWh	13.9 MWh
(249.4144, 461.0040)	9.3 MWh	9.0 MWh
(303.7968, 712.3305)	1.0 MW	0.7 MW
(157.0443, 499.1148)	0.5 MW	1.0 MW
(15.3938, 160.3585)	1.6 MW	1.4 MW

power production by the chillers with negligible cost increase. Indeed, the results obtained with the model for both design and optimization are very similar to the ones obtained with the model for design optimization. However, the savings obtained by optimal operation depend on the electricity cost, cost of equipment and number of cooling days. Electricity cost is highly uncertain, especially nowadays, as it can vary sensibly, as a response to market trends and geopolitical crisis. Equipment cost is also uncertain, as in literature it is common to find price ranges, but not the exact ones, which instead depend on many factors, such as the labor cost for installation, which varies from country to country. Lastly, the number of cooling days depends mainly on the climate zone.

In this section the results of a sensitivity analysis are presented. This is done to determine how these parameters influence the optimization results and how the operation strategy of chillers and storages changes with larger electricity costs, different costs for equipment installation. Hence, the analysis has been carried out on seven different scenarios, differing in terms of electricity cost profile, capital cost of centralized chillers or number of cooling days. Fig. 9 shows the electricity cost profiles considered for this analysis. *Scenario 0* indicates the standard scenario used in the previous simulations, while in *Scenario 1* and *Scenario 2* two different cost profiles were considered. *Scenario 1* is obtained increasing by 50 % the electricity cost of *Scenario 0*. *Scenario 2* was instead obtained by selecting a day of May 2022, in which it was observed a large peak of electricity cost and a wide difference between minimum and maximum electricity cost. This therefore does not represent a typical profile, observable every day, but it is rather an exception and an extreme situation that occurred during a period characterized by high electricity cost, due to different external geopolitical factors. *Scenario 2* therefore offers more opportunities for scheduling optimization. The two scenarios, named *Scenario 3* and *Scenario 4*, instead, are obtained by lowering or increasing the capital cost of chillers by 20 % with respect to *Scenario 0*. Lastly, *Scenario 5* and *Scenario 6* are obtained considering a larger number of cooling days and the cost profiles used in *Scenario 0* and *Scenario 2*, respectively. These two scenarios were considered as well, to determine how the results can differ if cooling demand is not seasonal. Table 8 summarizes the parameters used for all the seven scenarios.

6.1. Results

In the following subsections the optimal chillers and storages operation is presented for each of the new scenarios. In addition, Fig. 10 shows the comparison in terms of total costs between design only and

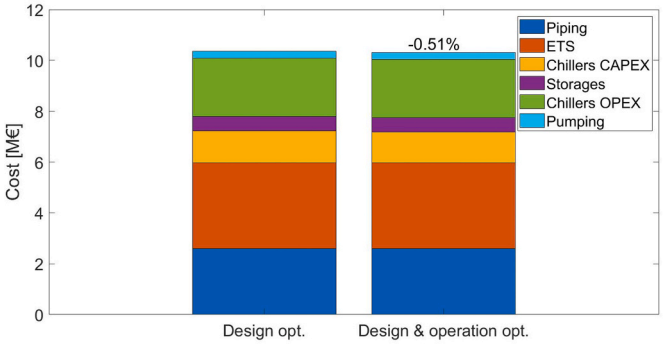

Fig. 8. Cost comparison between the optimal solutions obtained by the different models.

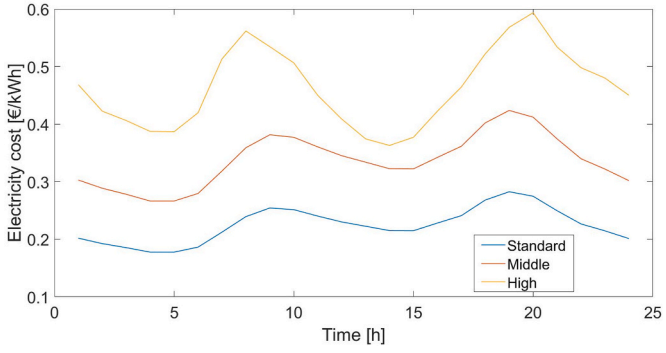

Fig. 9. Electricity cost profiles taken into account.

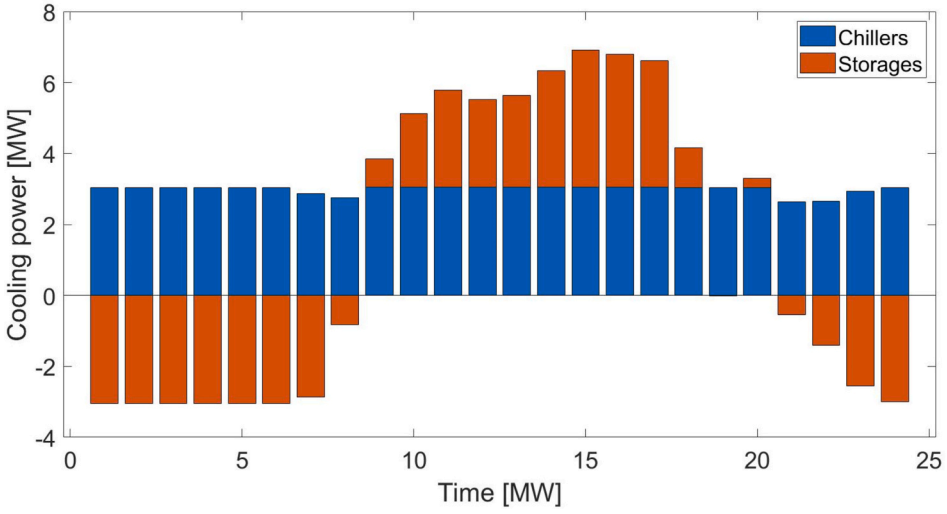

Fig. 7. Optimal chillers and storages hourly scheduling.

Table 8
Summary of scenarios.

Scenario	Electricity cost profile	Capital cost of centralized chillers	Number of cooling days
0	Standard (January 2022)	400 €/kW	60
1	Middle (January 2022 + 50 %)	400 €/kW	60
2	High (May 2022)	400 €/kW	60
3	Standard (January 2022)	320 €/kW	60
4	Standard (January 2022)	480 €/kW	60
5	Standard (January 2022)	400 €/kW	300
6	High (May 2022)	400 €/kW	300

combined optimization model solutions for all the new scenarios.

6.1.1. Scenario 1

Fig. 11 reports the hourly chiller and storage operation for scenario 1, obtained through the model for optimal design and operation. In this case, the chillers tend to operate almost constantly during the whole day, apart from 8 a.m. and in the evening, when the production is sensibly lower. In particular, at 9 p.m. the cooling power produced by the chiller is minimum and equal to 2.15 MW, while the maximum is 3.14 MW. The ratio between average and peak cooling production is equal to 95 %, since the load is sensibly lower only in few hours, while for the rest of the day it is almost constant.

As shown in Fig. 10, for *Scenario 1* the design and operation optimization (MIQCP) model allows to save 0.34 % more in terms of total life cycle costs with respect to the solution obtained the design optimization (heuristic).

6.1.2. Scenario 2

Fig. 12 shows the optimal hourly operation according to the design and operation optimization model for scenario 2. In this case, the chillers operation tends to exploit more the variations of the electricity cost. The cooling power, indeed, ranges between 0.95 MW and 3.46 MW. Hence, compared to the Scenario 0, the installed chiller capacity is 11.6 % larger. On the other hand, the ratio between the average and peak cooling production (capacity factor) is 86 %.

Fig. 10 shows that in Scenario 2 the additional savings that the design and operation optimization model allow to achieve amount to 1 % with respect to design only optimization.

6.1.3. Scenario 3

Fig. 13 shows the optimal daily operation according to the design and operation optimization model for Scenario 3. Also in this case, the cooling production is almost constant during the day. In particular, only in the 2 h with highest cost of electricity, the production is lower than 2.1 MW, while for the remaining 22 h, the chillers operate constantly with a total load of 3.05 MW. The ratio between average and maximum load is 97 %.

Fig. 10 shows that in this scenario, optimizing simultaneously operation and design would allow to save 0.57 % more with respect to optimizing only the design.

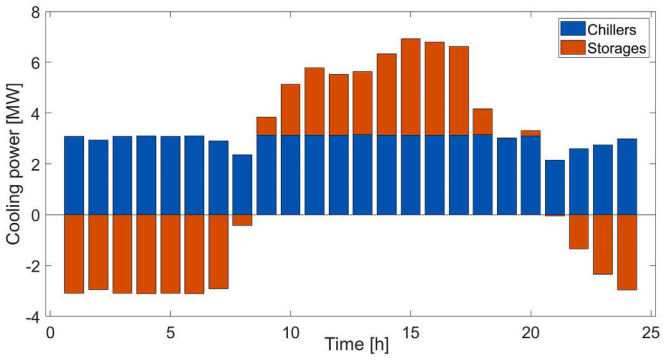

Fig. 11. Optimal chillers and storages hourly scheduling in scenario 1.

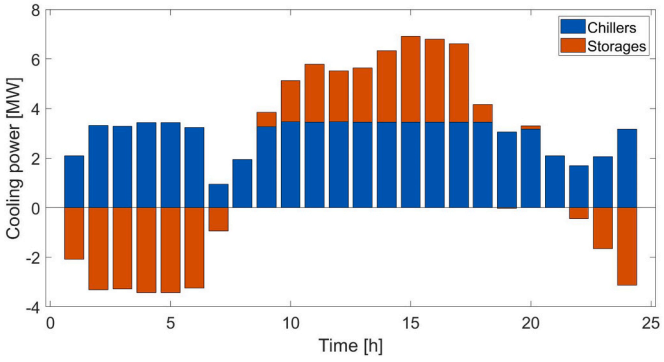

Fig. 12. Optimal hourly operation for scenario 2.

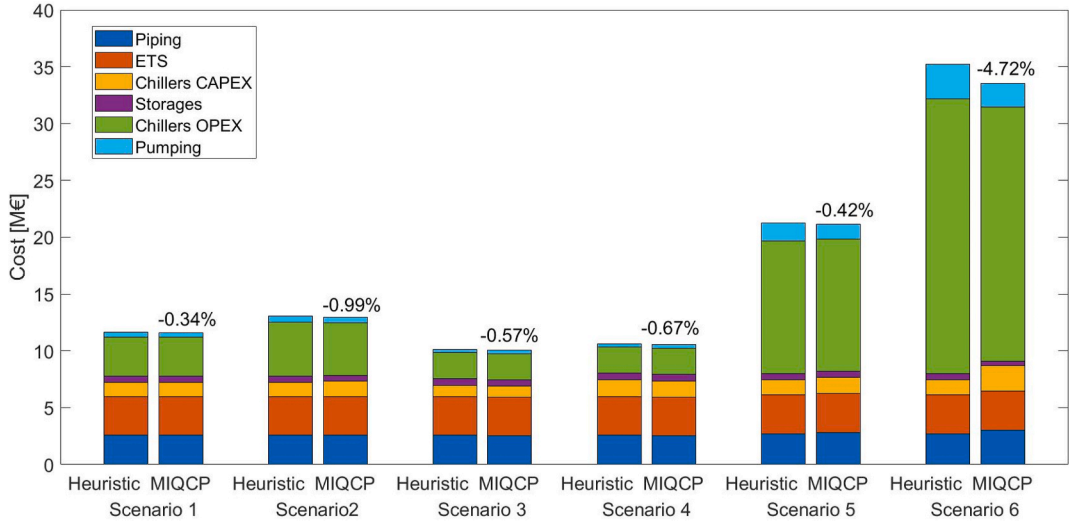

Fig. 10. Cost comparison between model solutions in different scenarios.

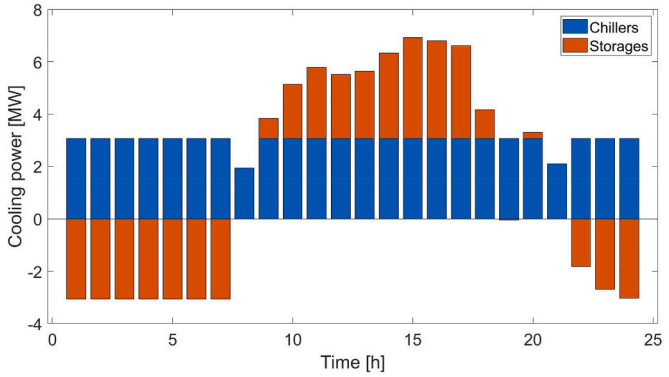

Fig. 13. Optimal operation in scenario 3.

6.1.4. Scenario 4

Fig. 14 shows the optimal schedule of chillers and storages according to the design and operation optimization model for Scenario 4. In this case, the chillers operate constantly, with a load of 2.99 MW, hence the ratio between average and maximum load is 100 %.

Fig. 10 shows that for Scenario 4, the design and operation optimization solution is 0.7 % less expensive, with respect to the one obtained by the design only optimization model. The reason for the difference, in this case is related to the assumption made in the design optimization model, for which the cooling production of chillers is discrete, rather than continuous, as it depends on the buildings that should be fed. The design and optimization model is instead more flexible, since the chillers can operate freely as long as the network energy and mass balances are respected.

6.1.5. Scenario 5

Fig. 15 shows the optimal dispatch of cooling power from chillers and storages for Scenario 5.

The maximum, minimum and average cooling power produced by the chillers are 3.54 MW, 1.61 MW and 3.04 MW, respectively. The chiller capacity factor is therefore 86 %, which is sensibly lower compared to scenario 0.

Fig. 10 shows that in this case, optimizing simultaneously operation and design allows to save 0.4 % more in terms of total life cycle costs.

6.1.6. Scenario 6

Fig. 16 shows the optimal daily operation for scenario 6. It can be observed that the chiller production is very discontinuous and not constant. The maximum cooling power produced by the chillers is 5.4 MW, with a capacity factor of 56 %.

From Fig. 10 it can be observed that in Scenario 6, characterised by the maximum fluctuation of electricity cost and days of use of the district cooling system, optimizing simultaneously design and operation allows

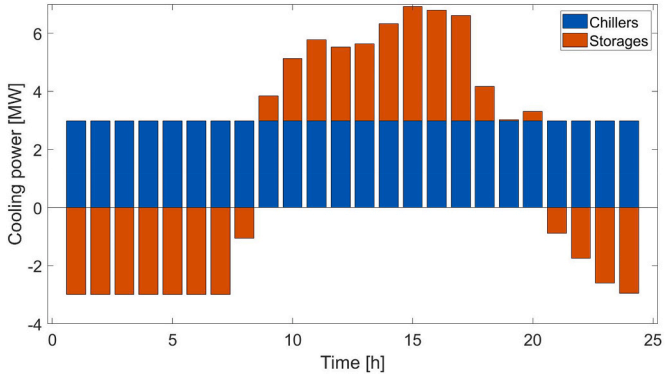

Fig. 14. Optimal hourly operation for scenario 4.

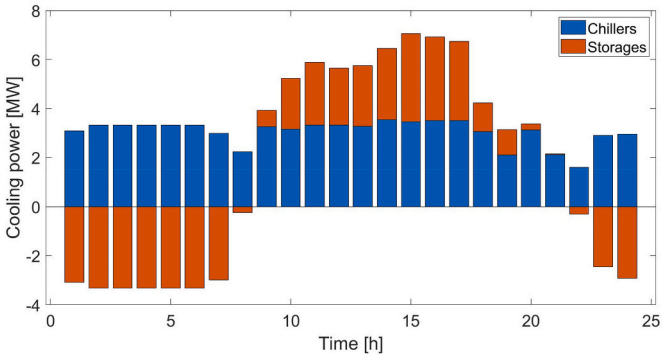

Fig. 15. Optimal hourly operation for scenario 5.

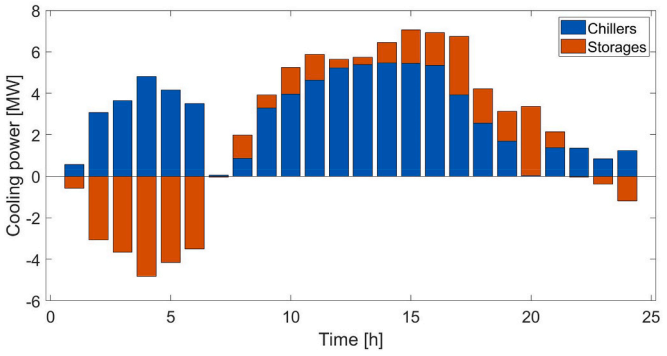

Fig. 16. Optimal hourly operation for scenario 6.

to save 4.7 % more with respect to optimizing only the design. It can also be observed that in the design and operation optimization solution the cost for chillers installation is higher, but this is compensated by lower cost of chillers operation and pumping.

7. Discussion

The design optimization model manages to optimize simultaneously the position of chillers and storages and the set of buildings to be connected, while keeping the computational time low, thanks to the combination of the iterative algorithm and the clustering approach. The chillers load is assumed to be constant and equal to the average cooling demand, minimizing the sizes. Hence in case of larger electricity costs, with daily fluctuations, the model may provide non-optimal results, as it optimizes only the design. On the other hand, the sensitivity analysis showed that if cooling demand is seasonal, even with larger volatility in the electricity prices, the relative difference in terms of objective function from the optimum found with a design and operation optimization model is around 1 %. By lowering the optimality gap of the design and operation optimization model, its solution may improve and the difference between the two models could rise, theoretically up to 3 %. Nevertheless, lowering the optimality gap would require a larger computational time and it is not guaranteed that a better solution will be found. Indeed, the optimality gap may be reduced by either improving the solution or by finding a new lower limit of the theoretical global optimum.

The design and operation optimization model managed to optimize both the size of the equipment and the operating schedule. If on one hand the model is more accurate than the first one, on the other hand it is highly computationally expensive, due to the complexity and presence of non-linearities. Moreover, it requires the electricity cost profile as an input, which is uncertain as well and may change in the future. However, the model could be useful to select suitable equipment sizes, on the basis of predictions on future energy prices.

The applicability of both models depends on the assumptions under which they are built. In particular, it is limited to tree-shaped networks. However, in case of looped networks, it could be possible to find equivalent tree-shaped networks, as shown in Ref. [21]. Moreover, since thermal losses and temperature evolution are neglected, in the case of uninsulated pipes, the models could slightly underestimate the operation costs. On the other hand, if the networks are relatively small and the temperature difference between the chilled water and the ground is sufficiently low, these phenomena can be neglected without sensible losses in accuracy. Additionally, the models assume a constant Energy Efficiency Ratio (EER), which is suitable for systems with constant supply chilled water and stable outdoor conditions. In the case of non-constant condenser temperatures, due to thermal excursion, these can be still taken into account by both models, considering a daily curve of EER. In that case, larger differences between the two models would be expected, due to the higher EER of chillers during the night.

The results obtained for scenarios from 0 to 4, show that the scheduling optimization of the district cooling network does not influence the design, hence operation and design optimization problems can be separated. The priority is to minimize the capital expenditures, which represent most of life cycle costs. The optimal solution suggests, indeed, to operate the chillers at constant load, minimizing in this way the capital costs, since pipes and chillers would need smaller sizes due to the absence of peak load. Hence, the impact of operation optimization is negligible and optimizing simultaneously the operation and the design of a district cooling network is not necessary. Similar results are achieved with different electricity tariffs; with larger electricity price fluctuations, operation optimization may provide additional savings. The sensitivity analysis also showed that by lowering the chiller costs, the results do not change sensibly. The results hence confirmed that within the ranges of chiller and electricity costs considered in the sensitivity analysis, the size of chillers in district cooling systems can be chosen so that they can operate at constant load. The installation of larger chillers would be justified only for larger differences between peak and off-peak electricity prices. In that case, the operation savings would be larger and could compensate the larger initial investment. Further cost savings may be obtained by optimizing a wider time period. These results are indeed based on the optimization of a reference day, limiting the storage strategy to 24 h. By optimizing longer periods, seasonal storage strategies could be considered, but larger sizes would be required, which usually are limited due to space constraints in urban areas.

The sensitivity analysis also showed that if cooling demand is not seasonal but is present throughout the entire year (scenarios 5 and 6), as in tropical climates, the impact of optimizing simultaneously design and operation is higher. Indeed, in these cases the relative difference in terms of total costs between the two models can be as high as 4.7 % if there is sufficient difference between off-peak and peak tariffs. Hence, if cooling demand is not seasonal, the model that optimizes both design and operation would be more appropriate, especially if there is large volatility of electricity price.

8. Conclusions

In this paper two different optimization models for district cooling networks are proposed. The first is based on a genetic algorithm coupled with a clustering approach and optimizes simultaneously the set of users to be connected and the position of chillers and storages. The operating schedule of the system is not optimized, but constant chiller operation is assumed, with thermal energy storages that match the unbalance between cooling production and demand. The proposed approach allows to reduce the computational cost for achieving the solution. The second model has been formulated as a Mixed Integer Quadratic Constrained Programming and optimizes simultaneously design and operation, selecting the equipment size and the operating schedule that minimizes the total costs. The set of users to be connected and the network layout are inputs of this model. Both models could also have broader applications in the context of smart energy systems. They could be adapted to other district energy networks, such as district heating, and integrated with local energy sources, such as waste heat, by introducing additional equipment like heat pumps or absorption chillers.

The two models have been applied to a case study characterized by a seasonal demand and compared to each other, in order to determine the effective impact on the results of simultaneously optimizing design and operation. For this case study the results obtained by the two models are very similar and for a standard scenario, characterized by typical electricity prices, differ by 0.5 % in terms of life-cycle costs. However, the computational cost of the first model is negligible with respect to the second model, as it took less than 1 % of the computational time required for the combined optimization.

A sensitivity analysis was also performed to determine how the results differ in scenarios with larger volatility of electricity price and different cost for chiller installation. It was observed that also by lowering chillers cost by 20 %, the model tends to minimize their sizes and operate them with constant load.

With further price difference between peak and off-peak periods, the impact of operation optimization could increase. However, it would be difficult to predict the future daily fluctuations of electricity price long in advance. Hence, in the design phase of district cooling systems it would be reasonable to separate design and operation optimization, assuming a constant operating schedule, if cooling demand is mainly seasonal. As a consequence, the use of district cooling networks as power-to-cool is certainly a benefit of this technology, as it allows to stabilize the grid, by operating the chillers and storing the cooling energy when electricity is cheaper and demand is lower. However, the design should not be affected by these strategies, as they would not be profitable enough to justify the installation of larger equipment.

For climates in which there is a continuous demand for cooling during the year, the situation is different. Indeed, the sensitivity analysis showed that in scenarios characterized by the presence of cooling throughout the entire year and a large difference between peak and off-peak electricity tariffs, installing larger chillers with the goal of exploiting these tariff differences would allow to save up to 4.7 % of total costs.

Therefore, it can be concluded that in climates in which cooling demand is concentrated in few months, it is appropriate to optimize the design of a district cooling network and assume a constant operation schedule of the chillers. On the other hand, in tropical countries, where there is always demand for cooling, this assumption has a sensible impact on the total life cycle cost, if the volatility of electricity price is sufficiently large. In these cases, it would be therefore more appropriate to optimize simultaneously both design and operation.

Declaration of competing interest

The authors declare that they have no known competing financial interests or personal relationships that could have appeared to influence the work reported in this paper.

Data availability

The data that has been used is confidential.

Acknowledgements

This research was funded in the Program Agreement between the Italian National Agency for New Technologies, Energy and Sustainable Economic Development (ENEA) and the Ministry of Economic Development (now Ministry of Ecological Transition) for Electric System Research, in the framework of its Implementation Plan for 2019–2021. In particular, the activity is included in the Project 1.5 “Technologies, techniques and materials for energy efficiency and energy savings in the electrical end uses of new and existing buildings”, Work Package 4

"Integrated Energy Networks".

References

[1] Tutak M, Brodny J. Renewable energy consumption in economic sectors in the EU-27. The impact on economics, environment and conventional energy sources. A 20-year perspective. J Clean Prod Apr. 2022;345:131076. https://doi.org/10.1016/J.JCLEPRO.2022.131076.

[2] IEA. Cooling. Paris. 2021. Accessed: Sep. 03, 2022. [Online]. Available: https://www.iea.org/reports/cooling.

[3] IEA. The future of cooling. Paris. 2018. Accessed: Sep. 06, 2022. [Online]. Available: https://www.iea.org/reports/the-future-of-cooling.

[4] Santamouris M. Cooling the buildings – past, present and future. Energy Build Sep. 2016;128:617–38. https://doi.org/10.1016/J.ENBUILD.2016.07.034.

[5] Chow TT, Au WH, Yau R, Cheng V, Chan A, Fong KF. Applying district-cooling technology in Hong Kong. Appl Energy 2004;79(3). https://doi.org/10.1016/j.apenergy.2004.01.002.

[6] Gang W, Wang S, Xiao F, Gao DC. District cooling systems: technology integration, system optimization, challenges and opportunities for applications. Renew Sustain Energy Rev Jan. 2016;53:253–64. https://doi.org/10.1016/J.RSER.2015.08.051.

[7] Chan ALS, Chow TT, Fong SKF, Lin JZ. Performance evaluation of district cooling plant with ice storage. Energy 2006;31(14):2750–62. https://doi.org/10.1016/J.ENERGY.2005.11.022.

[8] Inayat A, Raza M. District cooling system via renewable energy sources: a review. Renew Sustain Energy Rev 2019;107. https://doi.org/10.1016/j.rser.2019.03.023.

[9] Jangsten M, Lindholm T, Dalenbäck JO. Analysis of operational data from a district cooling system and its connected buildings. Energy Jul. 2020;203:117844. https://doi.org/10.1016/J.ENERGY.2020.117844.

[10] Hunt JD, Nascimento A, Zakeri B, Barbosa PSF, Costalonga L. Seawater air-conditioning and ammonia district cooling: a solution for warm coastal regions. Energy 2022;254(Sep). https://doi.org/10.1016/j.energy.2022.124359.

[11] Saleh Abushamah HA, Skoda R. Nuclear energy for district cooling systems – novel approach and its eco-environmental assessment method. Energy 2022;250(Jul). https://doi.org/10.1016/j.energy.2022.123824.

[12] Østergaard PA, et al. The four generations of district cooling - a categorization of the development in district cooling from origin to future prospect. Energy Aug. 2022;253. https://doi.org/10.1016/j.energy.2022.124098.

[13] Shi Z, Fonseca JA, Schlueter A. Floor area density and land uses for efficient district cooling systems in high-density cities. Sustain Cities Soc Feb. 2021;65:102601. https://doi.org/10.1016/J.SCS.2020.102601.

[14] Čož TD, Kitanovski A, Poredoš A. Exergoeconomic optimization of a district cooling network. Energy Sep. 2017;135:342–51. https://doi.org/10.1016/J.ENERGY.2017.06.126.

[15] Hosseini SE. Transition away from fossil fuels toward renewables: lessons from Russia-Ukraine crisis. Future Energy May 2022;1(1):2–5. https://doi.org/10.55670/fpll.fuen.1.1.8.

[16] Zhen L, Lin DM, Shu HW, Jiang S, Zhu YX. District cooling and heating with seawater as heat source and sink in Dalian, China. Renew Energy Dec. 2007;32(15):2603–16. https://doi.org/10.1016/J.RENENE.2006.12.015.

[17] Sameti M, Haghighat F. Optimization approaches in district heating and cooling thermal network. Energy Build 2017;140. https://doi.org/10.1016/j.enbuild.2017.01.062.

[18] Powell KM, Cole WJ, Ekarika UF, Edgar TF. Optimal chiller loading in a district cooling system with thermal energy storage. Energy Feb. 2013;50(1):445–53. https://doi.org/10.1016/J.ENERGY.2012.10.058.

[19] Wang L, Lee EWM, Yuen RKK. A practical approach to chiller plants' optimisation. Energy Build Jun. 2018;169:332–43. https://doi.org/10.1016/J.ENBUILD.2018.03.076.

[20] Chiam Z, Easwaran A, Mouquet D, Fazlollahi S, Millás Jv. A hierarchical framework for holistic optimization of the operations of district cooling systems. Appl Energy Apr. 2019;239:23–40. https://doi.org/10.1016/J.APENERGY.2019.01.134.

[21] Guelpa E, Verda V. Compact physical model for simulation of thermal networks. Energy 2019;175. https://doi.org/10.1016/j.energy.2019.03.064.

[22] Cox SJ, Kim D, Cho H, Mago P. Real time optimal control of district cooling system with thermal energy storage using neural networks. Appl Energy Mar. 2019;238:466–80. https://doi.org/10.1016/J.APENERGY.2019.01.093.

[23] Nova-Rincon A, Sochard S, Serra S, Reneaume JM. Dynamic simulation and optimal operation of district cooling networks via 2D orthogonal collocation. Energy Convers Manag Mar. 2020;207:112505. https://doi.org/10.1016/J.ENCONMAN.2020.112505.

[24] Yan B, Chen G, Zhang H, Wong MC. Strategical district cooling system operation with accurate spatiotemporal consumption modeling. Energy Build Sep. 2021;247:111165. https://doi.org/10.1016/J.ENBUILD.2021.111165.

[25] Zhang W, Hong W, Jin X. Research on performance and control strategy of multi-cold source district cooling system. Energy Jan. 2022;239. https://doi.org/10.1016/j.energy.2021.122057.

[26] Dominković DF, et al. Potential of district cooling in hot and humid climates. Appl Energy Dec. 2017;208:49–61. https://doi.org/10.1016/J.APENERGY.2017.09.052.

[27] Matak N, Tomić T, Schneider DR, Krajačić G. Integration of WtE and district cooling in existing Gas-CHP based district heating system – central European city perspective. Smart Energy Nov. 2021;4:100043. https://doi.org/10.1016/J.SEGY.2021.100043.

[28] Ismaen R, el Mekkawy TY, Pokharel S, Al-Salem M. System requirements and optimization of multi-chillers district cooling plants. Energy May 2022;246. https://doi.org/10.1016/j.energy.2022.123349.

[29] Chan ALS, Hanby VI, Chow TT. Optimization of distribution piping network in district cooling system using genetic algorithm with local search. Energy Convers Manag Oct. 2007;48(10):2622–9. https://doi.org/10.1016/J.ENCONMAN.2007.05.008.

[30] Zeng J, Han J, Zhang G. Diameter optimization of district heating and cooling piping network based on hourly load. Appl Therm Eng Aug. 2016;107:750–7. https://doi.org/10.1016/J.APPLTHERMALENG.2016.07.037.

[31] Egberts P, Tümer C, Loh K, Octaviano R. Challenges in heat network design optimization. Energy Jul. 2020;203:117688. https://doi.org/10.1016/J.ENERGY.2020.117688.

[32] Dobersek D, Goricanec D. Optimisation of tree path pipe network with nonlinear optimisation method. Appl Therm Eng 2009;29(8–9). https://doi.org/10.1016/j.applthermaleng.2008.07.017.

[33] Al-Noaimi F, Khir R, Haouari M. Optimal design of a district cooling grid: structure, technology integration, and operation. Eng Optim 2019;51(1). https://doi.org/10.1080/0305215X.2018.1446085.

[34] Dorfner J, Krystallas P, Durst M, Massier T. District cooling network optimization with redundancy constraints in Singapore. Future Cities and Environment Jan. 2017;3:1. https://doi.org/10.1186/s40984-016-0024-0. 0.

[35] Allen A, Henze G, Baker K, Pavlak G. Evaluation of low-exergy heating and cooling systems and topology optimization for deep energy savings at the urban district level. Energy Convers Manag Oct. 2020;222:113106. https://doi.org/10.1016/J.ENCONMAN.2020.113106.

[36] Allen A, Henze G, Baker K, Pavlak G, Long N, Fu Y. A topology optimization framework to facilitate adoption of advanced district thermal energy systems. IOP Conf Ser Earth Environ Sci Nov. 2020;588(2):022054. https://doi.org/10.1088/1755-1315/588/2/022054.

[37] Unternährer J, Moret S, Joost S, Maréchal F. Spatial clustering for district heating integration in urban energy systems: application to geothermal energy. Appl Energy Mar. 2017;190:749–63. https://doi.org/10.1016/J.APENERGY.2016.12.136.

[38] Yan R, Wang J, Zhu S, Liu Y, Cheng Y, Ma Z. Novel planning methodology for energy stations and networks in regional integrated energy systems. Energy Convers Manag Feb. 2020;205:112441. https://doi.org/10.1016/J.ENCONMAN.2019.112441.

[39] Chow TT, Chan ALS, Song CL. Building-mix optimization in district cooling system implementation. Appl Energy Jan. 2004;77(1):1–13. https://doi.org/10.1016/S0306-2619(03)00102-8.

[40] Bordin C, Gordini A, Vigo D. An optimization approach for district heating strategic network design. Eur J Oper Res Jul. 2016;252(1):296–307. https://doi.org/10.1016/J.EJOR.2015.12.049.

[41] Neri M, Guelpa E, Verda V. Design and connection optimization of a district cooling network: mixed integer programming and heuristic approach. Appl Energy 2022;306. https://doi.org/10.1016/j.apenergy.2021.117994.

[42] Dominković DF, Krajačić G. District cooling versus individual cooling in urban energy systems: the impact of district energy share in cities on the optimal storage sizing. Energies Jan. 2019;12(3):407. https://doi.org/10.3390/EN12030407. 2019, Vol. 12, Page 407.

[43] Alghool DM, Elmekkawy TY, Haouari M, Elomri A. Optimization of design and operation of solar assisted district cooling systems. 2020. https://doi.org/10.1016/j.ecmx.2019.100028.

[44] Guelpa E, Bellando L, Giordano A, Verda V. Optimal configuration of power-to-cool technology in district cooling systems. Proc IEEE Sep. 2020;108(9):1612–22. https://doi.org/10.1109/JPROC.2020.2987420.

[45] Wang H, Lahdelma R, Wang X, Jiao W, Zhu C, Zou P. Analysis of the location for peak heating in CHP based combined district heating systems. Appl Therm Eng Aug. 2015;87:402–11. https://doi.org/10.1016/J.APPLTHERMALENG.2015.05.017.

[46] Khir R, Haouari M. Optimization models for a single-plant district cooling system. Eur J Oper Res 2015;247:648–58. https://doi.org/10.1016/j.ejor.2015.05.083.

[47] Swedblom M, Mattson P, Tvärne A, Frohm H, Rubenhag A. District Cooling and the customers' alternative cost. 2014.

[48] Hauer A. Thermal energy storage. Accessed: Oct. 16, 2023. [Online]. Available: https://iea-etsap.org/E-TechDS/PDF/E17IR%20ThEnergy%20Stor_AH_Jan2013_final_GSOK.pdf; 2013.

[49] Martin-Candilejo A, Santillán D, Garrote L. Pump efficiency analysis for proper energy assessment in optimization of water supply systems. Water Dec. 2019;12(1):132. https://doi.org/10.3390/W12010132. 2020, Vol. 12, Page 132.

[50] Grygorash O, Yan Z, Jorgensen Z. Minimum spanning tree based clustering algorithms. In: Proceedings - international conference on tools with artificial intelligence. ICTAI; 2006. p. 73–81. https://doi.org/10.1109/ICTAI.2006.83.

[51] Optimization Gurobi. Gurobi reference manual. 2023. Accessed: Oct. 17, 2023. [Online]. Available: https://www.gurobi.com.

[52] UNI EN ISO 52016-1. Energy performance of buildings - energy needs for heating and cooling, internal temperatures and sensible and latent heat loads - Part 1: calculation procedures. 2018.

[53] Gestore Mercati Energetici. Esiti MGP. Accessed: Sep. 06, 2022. [Online]. Available: https://www.mercatoelettrico.org/it/download/DatiStorici.aspx.